# Prenatal retinoid deficiency leads to airway hyperresponsiveness in adult mice

Felicia Chen,[1] Hector Marquez,[1] Youn-Kyung Kim,[2] Jun Qian,[3] Fengzhi Shao,[1] Alan Fine,[1] William W. Cruikshank,[1] Loredana Quadro,[2] and Wellington V. Cardoso[3]

[1]Pulmonary Center, Boston University School of Medicine, Boston, Massachusetts, USA. [2]Department of Food Science and Rutgers Center for Lipid Research, Rutgers University, New Brunswick, New Jersey, USA. [3]Columbia Center for Human Development, Department of Medicine, and Pulmonary Allergy and Critical Care Medicine, Columbia University Medical Center, New York, New York, USA.

**There is increasing evidence that vitamin A deficiency in utero correlates with abnormal airway smooth muscle (SM) function in postnatal life. The bioactive vitamin A metabolite retinoic acid (RA) is essential for formation of the lung primordium; however, little is known about the impact of early fetal RA deficiency on postnatal lung structure and function. Here, we provide evidence that during murine lung development, endogenous RA has a key role in restricting the airway SM differentiation program during airway formation. Using murine models of pharmacological, genetic, and dietary vitamin A/RA deficiency, we found that disruption of RA signaling during embryonic development consistently resulted in an altered airway SM phenotype with markedly increased expression of SM markers. The aberrant phenotype persisted postnatally regardless of the adult vitamin A status and manifested as structural changes in the bronchial SM and hyperresponsiveness of the airway without evidence of inflammation. Our data reveal a role for endogenous RA signaling in restricting SM differentiation and preventing precocious and excessive SM differentiation when airways are forming.**

## Introduction

Vitamin A deficiency (VAD) is the most common dietary deficiency in the developing world and is associated with increased infant mortality and morbidity (1–3). It has been clear for decades that retinoic acid (RA), the active metabolite of vitamin A (retinol, ROH), plays a vital role in organogenesis and homeostasis, particularly in the lung (4, 5). Altered vitamin A or RA status has been linked to defects in embryonic and postnatal pulmonary development as diverse as lung agenesis, tracheoesophageal fistula, and bronchopulmonary dysplasia (6–10). Numerous clinical studies have demonstrated a positive relationship between vitamin A status and lung function. There is increasing evidence of an association between VAD and airway hyperresponsiveness, defined as an exaggerated contraction of the bronchial smooth muscle (SM) in response to environmental or pharmacological stimuli (11–14). These studies have also shown that maternal VAD has a negative impact on postnatal lung function in children, which can be alleviated by proper supplementation during gestation (15, 16).

SM is a major component of vascular and visceral structures, including airways, and the mechanisms that control growth and differentiation of SM in the embryonic lung remain poorly understood. Airway SM originates from various sources, including mesenchymal cells of the developing lung during formation of the bronchial tree (17–20). During development, the airway SM is responsible for phasic contractility of the liquid-filled epithelial tubules and production of growth factors, both critical for normal lung growth (21, 22). Changes in structural and mechanical properties of airway SM are found in conditions such as asthma that lead to airway hyperresponsiveness, remodeling, and airflow obstruction (23, 24). Interestingly, low serum levels of vitamin A have been reported in children with persistent asthma, correlating with the severity of disease (11, 25). Although inflammation plays a key role in triggering or exacerbating these responses, there is strong evidence that airway hyperresponsiveness can be uncoupled from inflammation and, at least in part, can result from fundamental changes in the SM phenotype itself (26, 27). How vitamin A/RA signaling regulates the program of SM differentiation in the lung, however, is unclear. The role of RA-dependent prenatal events in this process has been difficult to explore, since in most animal models, disruption of RA signaling leads to embryonic or neonatal lethality (28, 29). Thus, there is a paucity of information about the impact of early exposure of the fetal lung to insufficient levels of vitamin A/RA in postnatal life.

In the process of identifying genome-wide RA targets in early lung development, we found an abnormal increase in the expression of SM markers associated with RA-deficient status. This intriguing observation led us to further investigate the impact of RA signaling in SM development and lung function during pre- and postnatal life. We used cell and organ cultures and animal models in vivo and combined pharmacologic, genetic, and dietary approaches to address this issue. Here, we provide evidence that during lung development, RA has a key role in restricting the SM differentiation program of the forming airways. Our data show that prenatal vitamin A/RA deficiency fosters the development of an aberrant SM phenotype in the murine airways, leading to adverse effects on lung structure and function lasting well into adulthood.

## Results

*RA signaling influences SM marker expression during early lung development.* Using pharmacologic and genetic models of RA deficiency and gene expression profiling, we previously identified an RA-dependent gene network in the embryonic foregut critical for lung formation (30–33). A large number of these genes were shown to be present in the mesoderm and to be associated with a repressive function in multiple pathways (33). Surprisingly, we found that genes typically associated with SM differentiation were overrepresented and significantly upregulated in RA-deficient foreguts

**Conflict of interest:** The authors have declared that no conflict of interest exists.
**Citation for this article:** *J Clin Invest.* 2014;124(2):801–811. doi:10.1172/JCI70291.

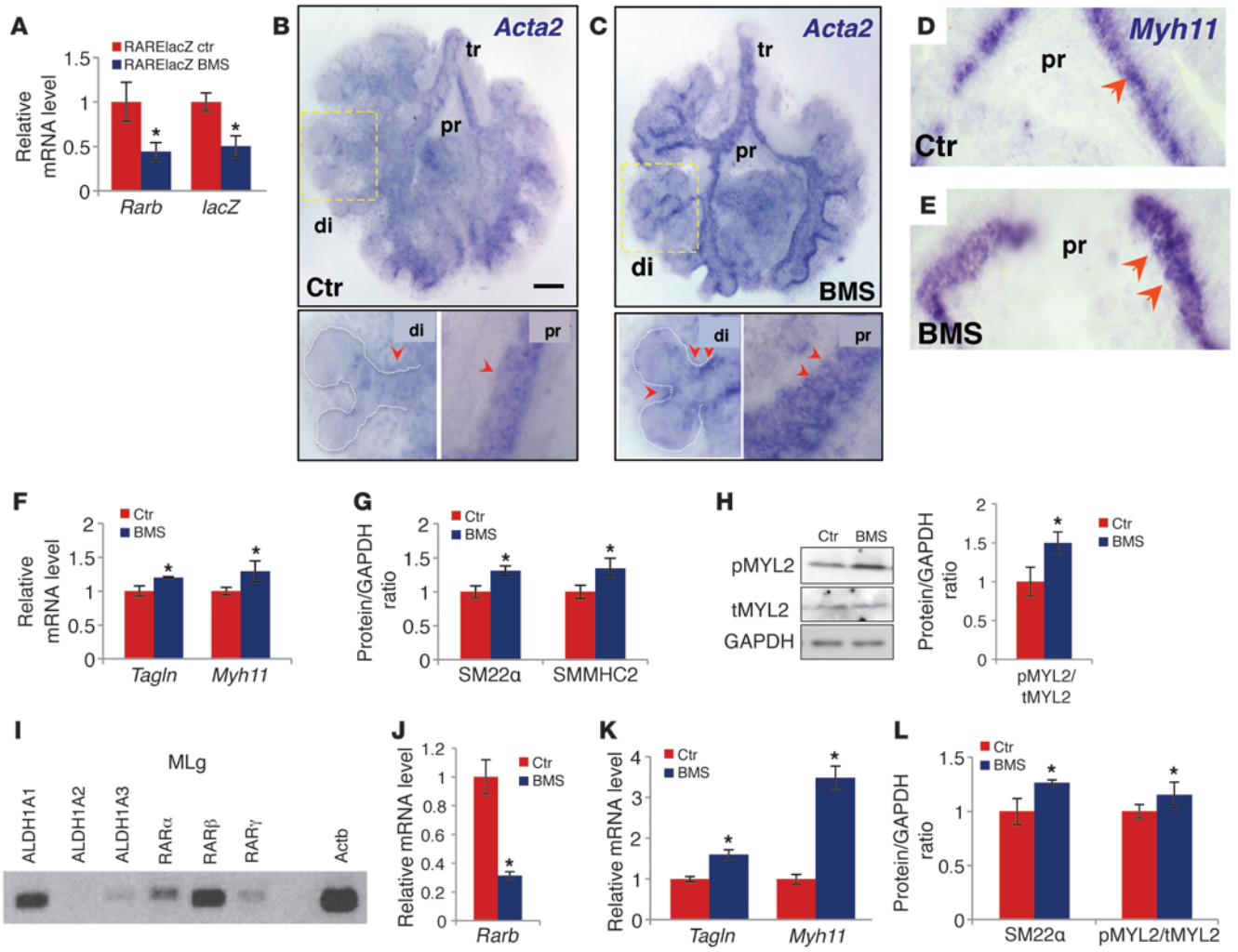


**Figure 1**

Disruption of RA signaling leads to aberrant expression of SM markers in mouse embryonic lung explant (**A**–**H**) and MLg cell (**I**–**L**) cultures. BMS-treated RARElacZ lungs (48 hours): significant downregulation of *Rarb* and *RARElacZ* (**A**) and increased expression of *Tagln* and *Myh11* (**F**) and their products SM22α and SMMHC2, respectively) (**G**). (**B**–**E**) Whole-mount ISH of *Acta2* (**B** and **C**) and *Myh11* (**D** and **E**) increased signals in the mesenchyme of proximal (pr) and distal (di) airways in BMS-treated lungs compared with those of controls (arrowheads). Strong ectopic *Acta2* expression was seen in stalks of distal buds in BMS-treated lungs. (**H**) Increased ratio of pMYL2/tMYL2 in BMS-treated lungs. (**I**) PCR detection of RA pathway components in MLg cells: RA-synthesizing enzymes (ALDH1A1, -2, and -3) and RA receptors (RARα, RARβ, and RARγ). (**J**–**L**) BMS treatment (24 hours) disrupted RA signaling (downregulation of *Rarb*) and increased expression of SM marker genes (*Tagln* and *Myh11*) and products (SM22α) and of the pMYL2/tMYL2 ratio. (**A**, **F**, **I**, and **K**) PCR and (**G**, **H**, and **L**) Western blot analysis. $n = 3–4$ per condition. $^*P < 0.05$. tr, trachea. Scale bar: 200 μm.

compared with those of the RA-sufficient controls. These included the following genes: actin, α 2, smooth muscle, aorta (*Acta2*); actin, γ 2, smooth muscle, enteric (*Actg2*); cysteine- and glycine-rich proteins 1 and 2 (*Csrp1* and *Csrp2*); transgelin (*Tagln*); myosin heavy chain 11, smooth muscle (*Myh11*); and calponin 2 (*Cnn2*) (ref. 34 and Supplemental Figure 1; supplemental material available online with this article; doi:10.1172/JCI70291DS1). These data raised the intriguing possibility that the RA status at a relatively early stage of lung organogenesis could influence and alter the program of mesenchymal differentiation.

To determine whether SM precursors in the embryonic lung are sensitive to changes in endogenous RA activation when airways are forming, we modulated RA signaling in lung explant cultures and examined the phenotype. E11.5 lungs from WT mice carrying one copy of the RA reporter *RARElacZ* were cultured for 48 hours under control conditions or in the presence of the RA receptor antagonist BMS493 (hereafter referred to as BMS) (35, 36). Disruption of RA signaling was confirmed by significant downregulation of *Rarb* and *lacZ* in BMS-treated lungs (Figure 1A); overall growth and patterning were unaffected. In situ hybridization (ISH) of SM marker genes, such as *Acta2* and *Myh11*, revealed a remarkable increase in signals in the mesenchyme associated with the developing airways of BMS-treated lungs compared with that seen in controls. Furthermore, expression of these genes extended ectopically to the stalk region of the most distal buds in the BMS-treated lungs (Figure 1, B–E).

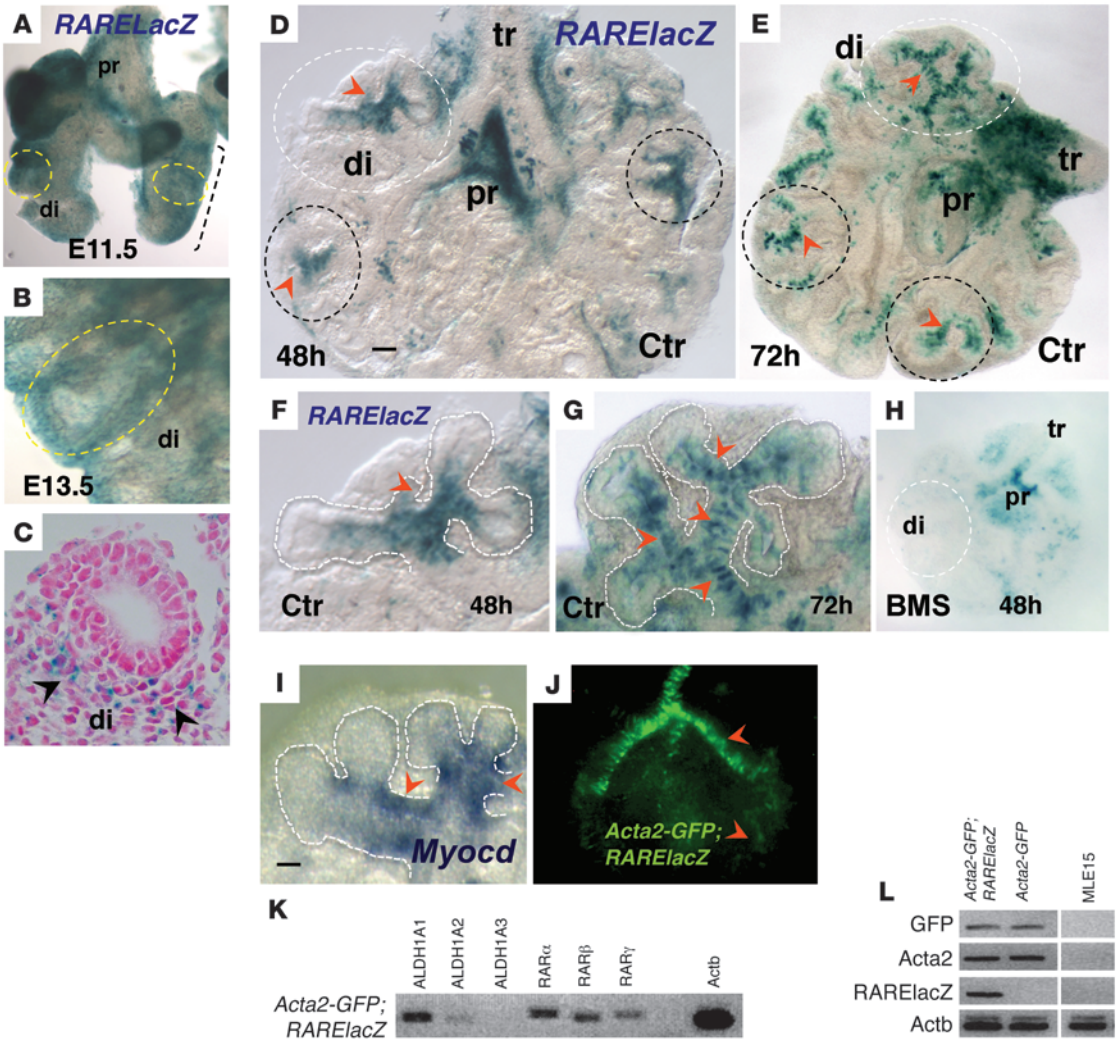


**Figure 2**

RA is active at sites of SM differentiation in developing distal airways. (**A**–**C**) X-gal staining of E11.5 (**A**) and E13.5 (**B** and **C**) *RARElacZ* lungs; mesenchymal signals were prominent in the distal lung (di, circled). (**C**) Cross section of E13.5 lung. (**D**–**H**) X-gal staining of cultured lung (48 and 72 hours). Strong local RA activity in the mesenchyme at the stalks of forming buds was seen at 48 hours (**D** and **F**, arrowheads; circled areas). At 72 hours, the pattern was more prominent, with multiple areas of *RARElacZ* labeling the mesenchyme associated with newly formed distal airways (**E** and **G**). Signals declined or were undetectable in more proximal branches, although they were present in trachea and main bronchi, being abolished by BMS treatment (**H**). Myocardin (*Myocd*) signals (ISH) were enriched in areas of strong RA activity (**I**, **F**, and **G**, arrowheads). (**J**–**L**) Lung culture from *Acta2-GFP;RARElacZ* mice showing GFP signals associated with airway SM (**J**). SM cells isolated by FACS expressed RA pathway components and activated RA signaling (**K** and **L**, PCR; negative controls: cells from *Acta-GFP*, non-*RARElacZ*, and MLE15 line). Scale bars: 55 μm (**D**) and 45 μm (**I**). $n$ = 3–5 per condition for all experiments.

The aberrant SM marker expression in these lungs was confirmed by a significant upregulation of *Tagln*, *Myh11* and their protein products (SM22α and SMMHC2, respectively), as revealed by quantitative real-time PCR (qPCR) and Western blot analysis (Figure 1, F and G). Since phosphorylation of myosin regulatory light chain 2 (MYL2) is required for SM contraction and its level correlates strongly with airway SM shortening velocity (37), the increase in phospho-MYL2 (pMYL2) over total MYL2 (tMYL2) in BMS-treated lungs suggests that the SM in these lungs is hypercontractile (Figure 1H).

To investigate whether the effect of RA signaling in the SM program was independent of signals originating from other cell types, we modulated signaling directly in the well-characterized mouse lung mesenchymal cell line MLg, which has previously been shown to have a response to RA similar to that of embryonic lung mesenchyme (33, 38). PCR analysis of RA pathway components revealed that under control conditions, MLg cells express the RA-synthesizing enzymes aldehyde dehydrogenase 1 family ALDH1A1, ALDH1A3, and ALDH1A2 (to a lesser extent) and RA receptors RARα, RARβ, and RARγ (Figure 1I). This suggests that they are able to produce active ligand from a retinoid precursor (in the media) and turn on RA signaling endogenously. Indeed, BMS treatment of MLg cells for 24 hours showed significantly lower levels of the early RA response gene *Rarb* compared with levels in cells

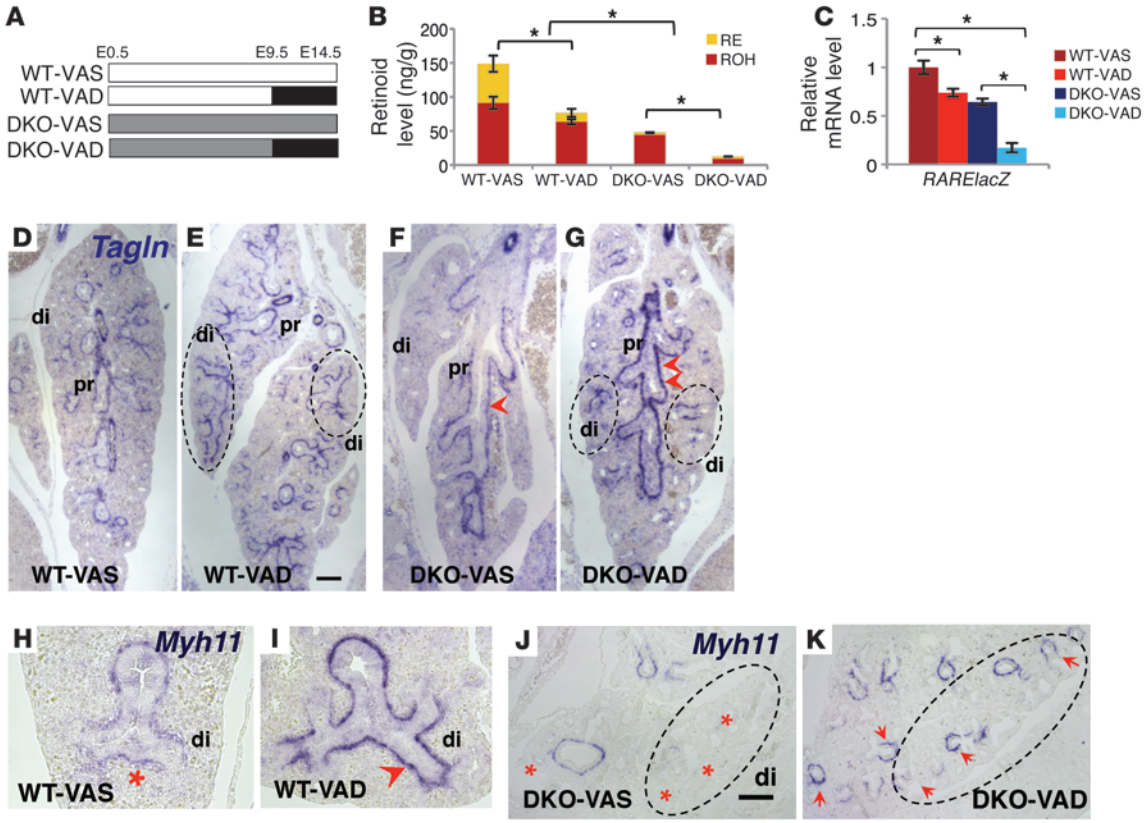


**Figure 3**

VAD in utero results in aberrant airway SM differentiation in E14.5 lungs. (**A**) Diagram of experimental design. (**B**) HPLC measurements of total retinoid (RE and ROH) in E14.5 lung homogenates (ng/g) from WT and DKO mice in VAS and VAD groups. (**C**) qPCR of *RARElacZ* expression in lung homogenates (all mice were bred into a RARElacZ line). (**D**–**K**) ISH of *Tagln* (**D**–**G**) and *Myh11* (**H**–**K**) showing increased expression of SM markers in the proximal airways of VAD lungs (arrowheads), most prominent in DKO VAD lungs (**G**). Ectopic expression extended to the most distal airways (circled regions) in the VAD groups (red asterisks denote no or low signals). $n = 6$ per condition. $^*P < 0.05$ compared with the VAS group. Scale bars: 150 μm (**E**) and 180 μm (**J**).

cultured under control conditions (Figure 1J). Consistent with the phenomenon seen in organ cultures, we observed that disruption of RA signaling led to an increased expression of SM markers both at the message and protein levels, as well as an increased pMYL2/tMYL2 ratio in these cells (Figure 1, K and L). Western blotting of Ki67, a marker of cellular proliferation, showed no difference between groups, suggesting a similar proliferative capacity (Supplemental Figure 2D). Thus, MLg cells seem to retain their capacity to activate endogenous RA signaling in the presence of a retinoid precursor and to control expression of SM markers on a per-cell basis.

Overall, our data suggest that the airway SM phenotype is strongly influenced by RA during lung development.

*RA is active in the developing SM layer of newly formed airways during branching.* The observations above prompted us to further investigate the relationship between activation of RA signaling and establishment of the SM program in forming airways. Previous analysis of the *RARElacZ* reporter showed that during branching morphogenesis, RA signaling becomes largely undetectable in the epithelium of forming buds. Signals are still maintained in the mesenchymal subpleural region and in mesenchymal derivatives, such as lymphatics, cartilage precursors, and some proximal epithelial cells (36, 39).

We performed X-gal staining of the embryonic lungs from a *RARElacZ* reporter mouse and confirmed the mesenchymal expression, which was particularly prominent in the distal lung (Figure 2, A–C). Diffuse mesenchymal signals were also present proximally in regions encompassing connective tissue and structures of the pulmonary hilum, such as large vessels and extrapulmonary airways, as previously reported (ref. 39 and data not shown). To better visualize how the mesenchymal pattern of RA activation is established in branching airways, we investigated the spatial distribution of *RARElacZ* in E11.5 lung explants growing under RA-sufficient (control) conditions. In these cultures, airway branching and differentiation can be easily followed, as the explant flattens and blood vessels, including vascular SM, do not develop. Our analysis of these explants up to 72 hours in culture revealed β-gal activity in a highly focal pattern in the subepithelial mesenchyme associated with the stalk region of the nascent buds (Figure 2, D–G). We found that the expression appeared to be dynamic, as it was most prominent in newly formed distal airways and was declining in preceding airway generations. This distal pattern of *RARElacZ* was highly dependent on endogenous RA, since it was completely abolished in BMS-treated cultures (Figure 2H).

Interestingly, the local sites of RA activation in the distal mesenchyme coincide with the sites of SM differentiation in newly formed airways (40–42). This was supported by the strong local expression of myocardin (*Myocd*), a serum response factor (SRF)

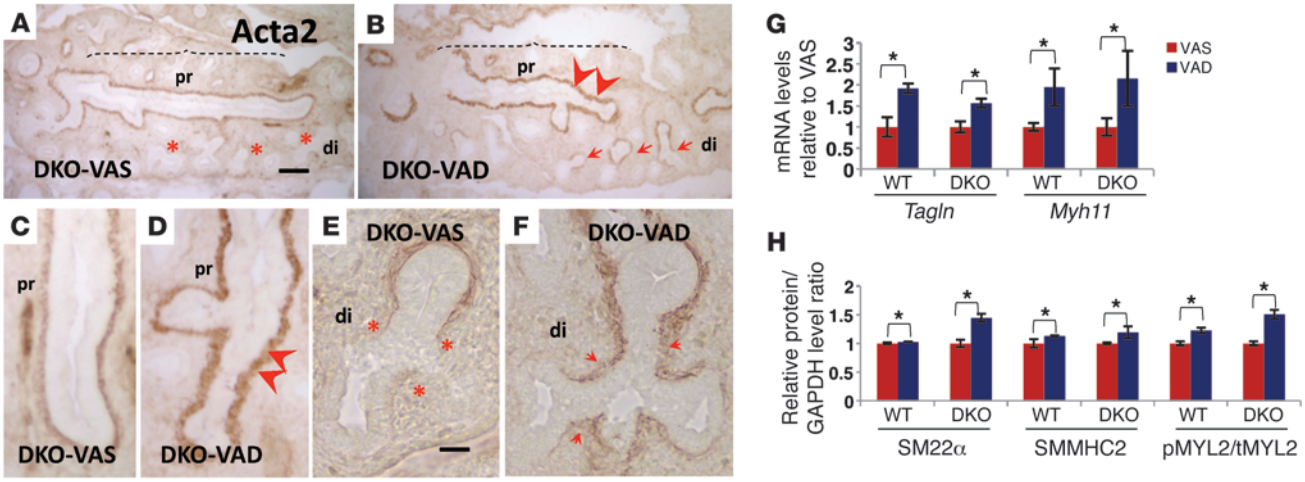


**Figure 4**

Aberrant airway SM differentiation in VAD E14.5 lungs. (**A**–**F**) Acta2 IHC in DKO lungs: an increased severity of the phenotype was seen in VAD lungs compared with that in VAS lungs. Stronger Acta2 signals were observed in the proximal airways, and ectopic Acta2 expression was seen in the distal airways of DKO-VAD lung. qPCR (**G**) and Western blot analysis (**H**) of SM markers and the pMYL2/tMYL2 ratio in lung homogenates confirm the aberrant SM differentiation when RA signaling was disrupted in vivo. $n = 6$ per condition. $^*P < 0.05$ compared with the VAS group. Scale bars: 135 μm (**A**) and 45 μm (**E**).

cofactor critical for regulation of SM-specific gene transcription as well as expression of myocardin-related factors, as previously reported (Figure 2I, data not shown, and refs. 43–45).

To further investigate the presence of RA activity in SM cells of the developing lung, we crossed *RARElacZ* mice with an *Acta2-GFP* reporter mouse line, in which GFP is expressed under the control of the rat *Acta2* promoter (46). GFP-positive cells isolated and sorted from E13.5 *Acta2-GFP* lungs (not shown) and lung explant cultures (Figure 2J) expressed RA pathway components, including key RA-synthesizing enzymes ALDH1A1 and ALDH1A2 and RA receptors RARα, RARβ, and RARγ. Furthermore, GFP-positive cells from *Acta2-GFP*;*RARElacZ* double-transgenic lungs expressed *lacZ* by PCR analysis (Figure 2, K and L), confirming the presence of RA signaling in SM cells of the embryonic lung. The observations above and the results from our functional assays in organ and cell culture were consistent with the hypothesis that endogenous RA restricts SM differentiation in the distal lung.

*VAD in utero results in aberrant airway SM differentiation during development in vivo*. We asked whether the SM phenotype observed in lung cell and organ cultures could also occur in vivo. Thus, we investigated the impact of maternal VAD in the development of airway SM in the embryonic lung. We disrupted RA signaling by restricting maternal vitamin A dietary intake and by using a mouse mutant strain lacking both *Lrat* (lecithin retinol acyltransferase) and *Rbp4* (retinol-binding protein 4, plasma) genes. LRAT is the main enzyme required for the formation of retinyl esters (RE), the storage form of vitamin A, in both adult and developing tissues; RBP4 is the sole specific transport protein for ROH in the bloodstream. Being unable to store vitamin A or to mobilize it from the liver as RBP4-bound retinol, these mice rely on dietary vitamin A to support their retinoid-dependent functions, such as embryogenesis (47). *Rbp4;Lrat* double-null (hereafter referred to as DKO) mutants on a normal vitamin A–sufficient (VAS) diet have negligible RE levels and substantially lower ROH levels than WT mice, but do not show the developmental defects or lethality of severely RA-deficient mice unless fed a VAD diet (<0.2 IU vitamin A/g) from the earliest developmental stages. Thus, DKO mice have been used as a tunable model of vitamin A/RA deficiency. Since these animals have chronically low retinoid levels despite a VAS diet, they also serve as a model of mild chronic VAD when compared with WT mice (47).

We characterized SM development in E14.5 lungs from WT and DKO embryos whose mothers were fed a VAS diet throughout life or a VAD diet from gestation days E9.5 to E14.5 (Figure 3A). This window of VAD was selected because it encompasses the initial stages of lung morphogenesis and airway SM development (41, 48) and prevents early embryonic lethality (47). Reverse HPLC analysis was used to determine RE and ROH levels in embryonic lungs (ref. 49 and Figure 3B). WT embryos responded to the maternal VAD diet by exhibiting lower ROH and RE contents in the lung ($P < 0.05$). We found that lungs from DKO mice showed a major reduction in ROH content compared with that in seen WT mice, with DKO-VAD mice being the most severely affected. RE was nearly undetectable in both DKO-VAS and DKO-VAD lungs, consistent with the critical role of LRAT in RE formation.

We then generated reporter lines to assess overall RA activity in these lungs by breeding WT or DKO mice with *RARElacZ* mice. Decreased *lacZ* expression, as demonstrated by qPCR in lung homogenates of E14.5 WT;*RARElacZ* VAD, DKO;*RARElacZ* VAS, and DKO;*RARElacZ* VAD mice relative to that in WT;*RARElacZ* VAS mice, confirmed the downregulation of RA signaling (Figure 3C). Remarkably, ISH of E14.5 lungs from DKO embryos showed a thicker layer of subepithelial mesenchymal cells in the proximal airways expressing *Tagln* and *Myh11* compared with that seen in WT lungs. The aberrant expression of SM markers in proximal airways was most severe in the DKO-VAD embryos (Figure 3, D–G). Furthermore, we found that a maternal VAD diet in both WT and DKO embryos resulted in a strong ectopic expression of *Tagln* and *Myh11* that extended to the most distal airways (Figure 3, D–J). We observed that both proximal and distal features of the aberrant phe-

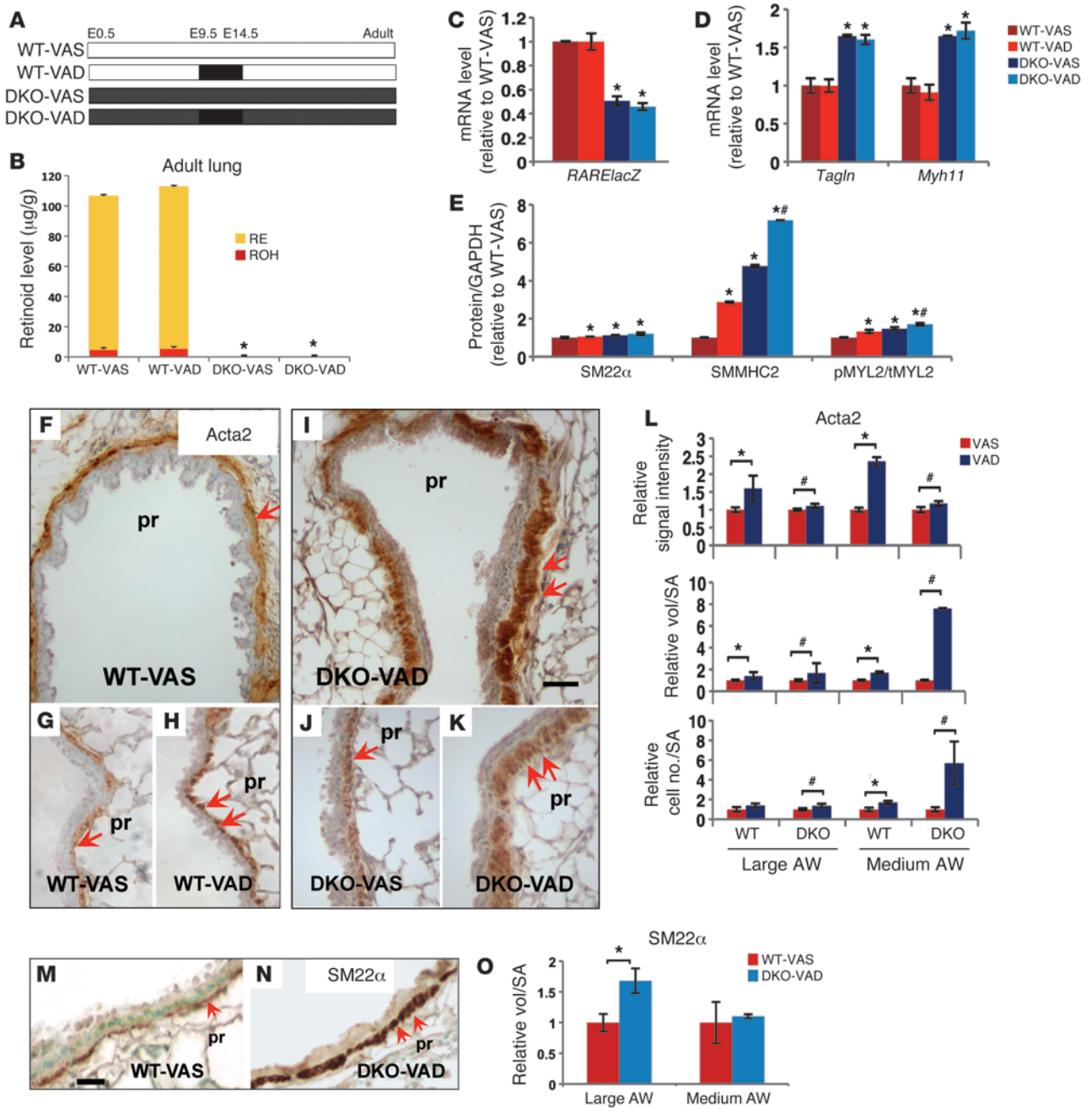


**Figure 5**

Consequences of prenatal VAD in the SM phenotype of the adult lung. (**A**) Diagram of experimental design. (**B**) HPLC measurements of retinoids in the lung homogenates of adult mice: no difference between VAS and VAD groups, but significantly lower levels in DKO compared with WT mice. (**C**–**E**) Significantly lower levels of RARElacZ (**C**) correlating with *Tagln* and *Myh11* upregulation (**D**) by qPCR in DKO lungs compared with WT. (**E**) Significant increase in SM22α, SMMHC2, and pMYL2/tMYL2 ratio levels in lung homogenates of WT-VAD, DKO-VAS, and DKO-VAD mice compared with those in WT-VAS lung homogenates by Western blot analysis. IHC of SM markers in adult proximal airways (**F**–**K**: Acta2; **M**–**N**: Sm22α) showing increased expression in VAD groups (double arrows). Quantitative analysis of Acta2 (**L**) and Sm22α (**O**) IHC: signal intensity, relative volume of staining per SA, and relative number of labeled cells per SA in proximal airways (large and medium size, see Methods) suggest a significant increase in SM mass in VAD lungs relative to VAS lungs. Data represent the mean ± SEM, $n = 3$ per condition. $^{*}P < 0.05$ compared with WT-VAS; $^{\#}P < 0.05$ compared with DKO-VAS. Scale bars: 30 μm (**I**) and 20 μm (**M**). AW, airway.

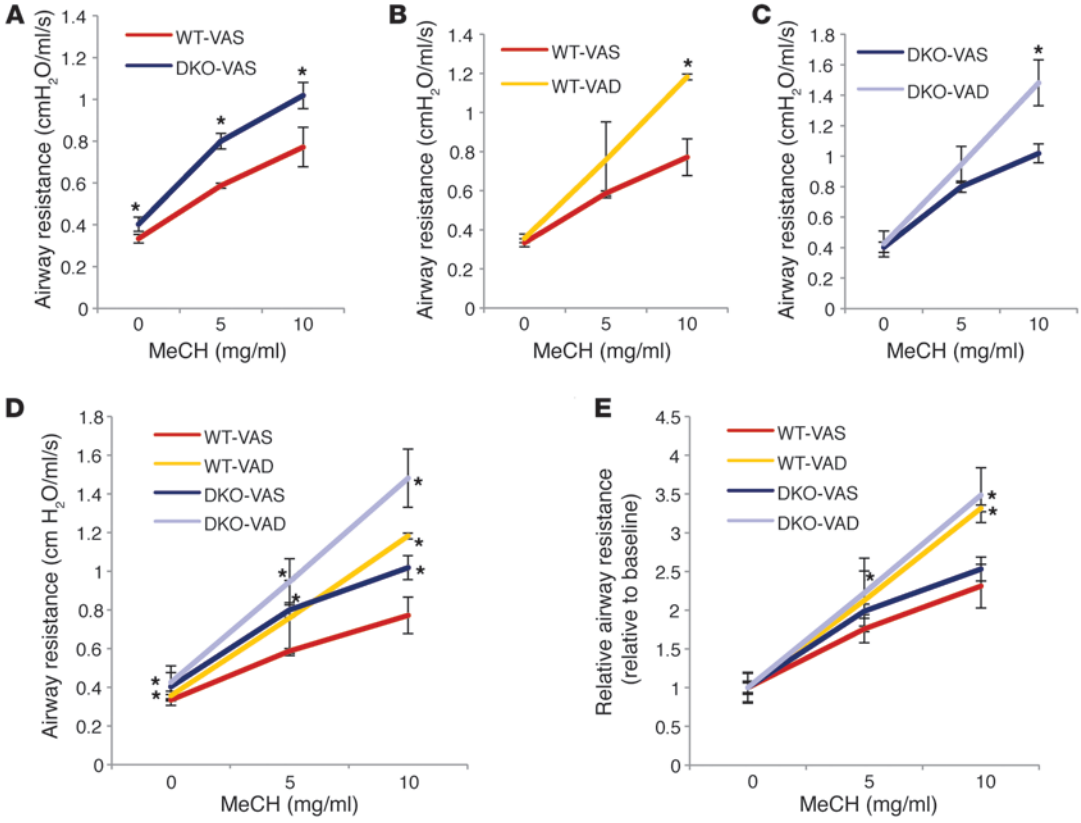


**Figure 6**

Prenatal VAD results in increased airway responsiveness in adulthood. flexiVent analysis of airway resistance in a nonchallenged state and in response to methacholine (MeCH). (**A**) Airway resistance of DKO-VAS adult mice was higher than that of WT-VAS adult mice at baseline and at all doses of methacholine. (**B** and **C**) VAD mice showed increased response to methacholine compared with that of VAS groups in both WT (**B**) and DKO (**C**) mice. (**D**) Both WT and DKO mice subjected to a prenatal VAD diet had the highest response to methacholine at 10 mg/ml. (**E**) Relative airway resistance (absolute resistance normalized by baseline value): differences between DKO and WT mice were minimized, but differences between VAS and VAD mice persisted. *$P < 0.05$ compared with WT-VAS ($n = 4$ DKO-VAS; $n = 3$ for other conditions).

notypes were also evident by Acta2 immunohistochemistry (IHC) of DKO-VAD lungs compared with DKO-VAS lungs (Figure 4, A–F, and Supplemental Figure 2, A–C). qPCR and Western blot analyses of SM markers confirmed the increase in *Tagln*, *Myh11*, SM22α, and SMMHC2 as well as in the pMYL2/tMYL2 ratio, correlating inversely with retinoid content and RA activity in these lungs (Figure 4, G and H). We found that the changes in the SM phenotype were not accompanied by differences in cell proliferation, as assessed by Ki67 or PCNA staining (Supplemental Figure 2, E–J). Moreover, the pattern of SM gene expression in lung blood vessels was essentially the same in all groups (Supplemental Figure 4, A and B). We detected no gross morphological abnormalities in these mice other than a slight decrease in the size of the DKO embryos and lungs compared with those of WT animals. IHC staining of SRY-BOX 2 (SOX2) and SRY-BOX 9 (SOX9), markers of proximal and distal lung epithelium, respectively (50–52), showed no difference in proximal-distal (P-D) patterning among groups (Supplemental Figure 3).

Overall, our data suggest that prenatal VAD profoundly alters the airway SM differentiation program in vivo.

*The abnormal SM phenotype due to prenatal VAD is carried throughout life and is prominent in the adult lung.* We asked whether the dramatic changes in SM observed in VAD airways during development could lead to a permanent phenotypic defect in the adult lung. We used DKO mice, which are viable and fertile when fed a VAS diet, to investigate the postnatal effects of the embryonic VAD diet. WT and DKO embryos were subjected to VAS or VAD regimens in utero, as described above. However, instead of being terminated on E14.5, embryos were allowed to develop to adulthood with a VAS diet (Figure 5A and Methods).

Reverse HPLC analysis of WT adult lungs showed RE as the predominant form of retinoid. Lungs from all DKO adult mice had a markedly lower level of ROH compared with that in WT mice and essentially undetectable RE (Figure 5B). As expected, a VAD diet between E9.5 and E14.5 did not influence retinoid levels in either WT or DKO models. However, our analysis of the mutant mice carrying the *RARElacZ* transgene showed that the very low retinoid content in DKO adult lungs only reduced RA activity by approximately 50% (Figure 5C). We investigated the impact of this reduction in RA activity on the SM phenotype of adult DKO lungs. qPCR showed a 1.6- to 1.8-fold increase in *Tagln* and *Myh11* relative to that in WT lungs, suggesting that the chronic RA deficiency in DKO mice, although not severe, still influenced SM gene transcription (Figure 5D). The levels of SM22α and SMMHC2, as revealed by Western blot analyses, were significantly increased in the adult DKO lungs compared with levels in WT lungs. Notably, while lungs from VAS and VAD mice had similar levels of *Tagln* and

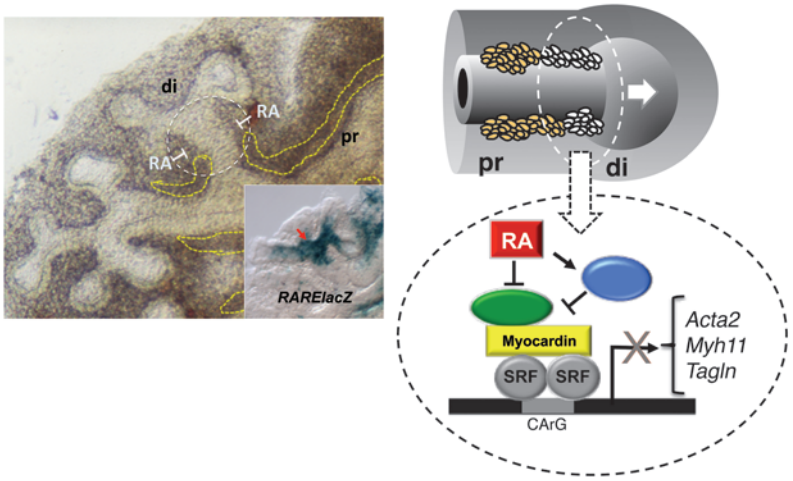


**Figure 7**
Proposed mechanism of SM regulation by endogenous RA. During branching of the developing airways, a program of differentiation of SM takes place in the distal mesenchyme at the newly formed stalks of the lung buds (white circled area). RA signaling is activated in these areas, as evidenced by locally enriched *RARElacZ* expression (inset) at these sites. Endogenous RA regulates this SM program, restricting SM gene expression and preventing excessive formation of SM while airways are branching. As new generations of airways arise, the process is reiterated, and the RA restriction of the SM program becomes less crucial proximally (left panel, dashed yellow lines). RA fine-tunes the SM gene expression program, likely by inhibiting the expression of a key activator of SM transcription (in green) or by inducing the expression of the transcriptional repressor (in blue), ultimately resulting in the downregulation of SM gene expression.

*Myh11* in each group, the protein products were increased in those exposed to a gestational VAD diet. The abnormal SM phenotype associated with fetal VAD exposure was further supported by the increased pMYL2/tMYL2 ratio in these lungs (Figure 5E).

Immunostaining and morphometric analyses of Acta2 (Figure 5, F–L) showed a marked increase in signal intensity, relative volume, and number of Acta2-labeled cells per surface area (SA) in large- and medium-sized airways of VAD versus VAS lungs. Terminal bronchioles of VAD lungs appeared unaffected, likely due to the limited exposure time to the VAD diet influencing only a few initial generations of branches. Analysis of Sm22α IHC showed similar findings (Figure 5, M–O). Vascular SM appeared to be unaffected by gestational VAD status, consistent with our previous observations in E14.5 lungs (Supplemental Figure 4, A and B). Importantly, the SM abnormalities from the embryonic VAD exposure of WT mice (Figure 3, H and I) indicate that the aberrant SM phenotype is present despite normal adult RA status. Thus, prenatal disruption of RA signaling leads to long-lasting structural changes in the airways.

*Prenatal disruption of RA signaling results in increased postnatal airway responsiveness.* Increased airway SM mass and pMYL2/tMYL2 ratio correlate with increased SM contractility and responsiveness to bronchoconstrictive stimuli (24). We reasoned that the structural changes in the adult airway resulting from prenatal RA deficiency were accompanied by abnormal bronchial responsiveness. Thus, we assessed the degree of airflow obstruction in adult WT or DKO mice under VAS or gestational VAD conditions using a flexiVent ventilator. We measured airway resistance in a nonchallenged state (baseline) and in response to an increased concentration of a bronchoconstrictor (methacholine; 5 and 10 mg/ml) (53).

Remarkably, we found baseline airway resistance in DKO mice to be already significantly higher than that in WT mice, but no differences were seen between VAD and VAS mice in each model (Figure 6A). This supports the idea that a chronic low vitamin A status in the DKO mice leads to airway structural and functional changes that ultimately influence the basal tone of airway resistance.

When challenged with methacholine, mice that were subjected to the window of VAD diet in utero had an exaggerated response, with DKO-VAD mice showing the highest increase in airway resistance (Figure 6, A–D). When absolute airway resistance was normalized to the airway resistance of the unchallenged state in each group, thereby eliminating basal tone in the unchallenged state as a determinant of airway resistance, the differences between the WT and DKO groups were minimized, but the differences between the VAD and VAS groups were still evident (Figure 6E). Overall, the data support the hypothesis that insufficient levels of vitamin A prenatally predispose to airway hyperresponsiveness.

## Discussion

Studies in cell culture and injury models show that SM cells are highly diverse and plastic, with features ranging from a more mature phenotype characterized by an abundance of SM markers and contractile apparatus, to a less differentiated phenotype, marked by a tendency to proliferate and synthesize bioactive proteins and ECM. The balance of these phenotypes during development or injury/repair is largely dependent on environmental cues acting in a network of intracellular signals and, ultimately, phenotype-specific genes and their products (54). We have previously identified RA as a major regulatory signal integrating multiple pathways in the foregut to control formation of the lung primordium (30–33). Here, we provide evidence that during lung development, endogenous RA has an additional key role in restricting the SM differentiation program when airways are forming and branching. It is remarkable that disruption of RA signaling in all of the models examined here consistently resulted in upregulation of SM contractility markers. The developmental defect caused by prenatal RA deficiency appeared to result in an overall increase in airway SM mass that persisted throughout life and manifested in the adult as abnormal airway SM accumulation and hyperresponsiveness.

We had no evidence that the excess in airway SM in retinoid-deficient lungs resulted from excessive proliferation of SM cells. Instead, we speculate that this phenotype may arise from increased recruitment of putative mesenchymal precursors into the SM program or from uninhibited differentiation of cells already committed to the SM phenotype in newly formed airways. Our findings of RA pathway components and *RARElacZ* expression in *Acta2-GFP*–labeled cells favor the latter scenario. Future lineage studies can help clarify this issue. We propose that in the developing lung, endogenous RA maintains airway SM cells in a less differentiated state to prevent precocious and excessive SM differentiation while distal airways are forming (Figure 7). In this regard, the mechanism we describe is similar to that reported in the developing cor-

onary artery, where activation of RA signaling in SM precursors delays the program of SM differentiation to allow ECs to differentiate first and maintain orderly vascular morphogenesis (55).

Proper differentiation and patterning of airway SM require input from multiple pathways, including SHH, FGF, WNT, TGFβ, and BMP (41, 42, 48). Signaling by SHH, BMP4, NOTCH, WNT2B, or WNT7B induces SM differentiation in the lung mesenchyme (40, 56–60). By contrast, activation of FGF9/FGFR signaling suppresses SM differentiation in a mechanism that involves inhibition of *Myocd* expression (60). MYOCD and SRF are major components of a transcriptional complex that regulates SM cell–specific gene expression (45). Data from our qPCR analysis of lung explant and MLg cultures as well our microarray screen of RA targets in the foregut (32, 33) suggest that the inhibitory effect of RA on the SM program is unlikely to be mediated through changes in expression of MYOCD or SRF (not shown). RA fine-tunes the SM gene expression program presumably by inhibiting expression of a key activator of SM transcription or by inducing expression of the transcriptional repressor, ultimately resulting in downregulation of SM gene expression (Figure 7). Preliminary studies suggest that this mechanism may involve RA-dependent epigenetic modifications (H. Marquez, Y. Cao, F. Chen, and W.V. Cardoso, unpublished observations).

A link between VAD and increased airway responsiveness had been previously reported in adult rats exposed to a prolonged VAD diet after weaning (61). The airway hyperresponsiveness was attributed to the reduced expression and function of muscarinic acetylcholine receptor $M_2$ (*Chrm2*) and decreased elastic fibers in the interstitium, but there was no structural defect in the airway SM. Our study is fundamentally different in that the period of VAD is limited to a defined prenatal developmental window or starts from early prenatal life in the DKO mutants. We found major changes in SM structure and function, but no difference in *Chrm2* expression between groups (Supplemental Figure 4K). No obvious changes were detected in the lung parenchyma suggestive of airspace enlargement, alveolarization deficit, cellular inflammation, or excessive ECM deposition (Supplemental Figure 4, C–J). This was further supported by the similar elastance values from these lungs (Supplemental Figure 4L). Thus, in our models, it is unlikely that changes in the alveolar compartment contributed to the functional alterations described here.

How do the observations described here relate to those that link vitamin A and airway function in human studies? Epidemiological and experimental studies support the idea that adverse influences during development can cause lifelong changes in various organs, leading to increased risk of disease in adulthood (62). Relevant examples include the association between reduced lung function at birth and an increased risk of asthma later in life (63) and the link between maternal smoking and abnormal lung function in neonates (64). Furthermore, maternal VAD during pregnancy is now known to have a negative impact on postnatal lung function in the offspring (15).

We believe that the present study establishes for the first time that a brief period of VAD during pregnancy at a critical period of fetal development can lead to chronic airway hyperresponsiveness. Our observations are likely to have important implications for the understanding of airway diseases such as asthma, in which airway hyperresponsiveness is both a risk factor and a major component.

## Methods

*DKO, RARElacZ reporter, Acta2-GFP reporter, and Aldh1a2-null mice*. These mice were characterized previously and identified by PCR genotyping or Western blot analysis (28, 35, 47, 46). DKO;*RARElacZ* mice were generated by crossing DKO mice with *RARElacZ* reporter mice. The F1 progeny was subsequently bred with DKO mice to generate DKO;*RARElacZ* mice. *Acta2-GFP;RARElacZ* double reporters were generated by crossing *Acta2-GFP* mice with *RARElacZ* mice. RA pathway activation was detected by X-gal staining on *RARElacZ*-positive tissues (36). All mice used in this study were on a CD1 background. The *RARElacZ* reporter mouse line was a gift of Janet Rossant (University of Toronto, Toronto, Ontario, Canada). The *Aldh1a2*-null mouse line was provided by Pascal Dollé and Karen Niederreither (Université de Strasbourg, Illkirch, France).

*MLg cell cultures*. Mouse neonatal lung mesenchymal MLg cells (ATCC) were plated (10% FBS, 1% penicillin and streptomycin in MEM) at a density of $10^6$ cells per 100 $mm^3$. Cells were cultured in media with or without pan-RAR antagonist BMS493 ($10^{-6}$ M; Sigma-Aldrich) for 24 hours and then processed for qPCR or Western blot analysis.

*Foregut and lung explant cultures*. Foreguts isolated from 8- to 12-somite E8.5 embryos were cultured for 24 hours at 37°C in 5% $CO_2$ on 6-well Transwell-COL dishes (Fisher Scientific) containing 1.5 ml BGJb medium (Invitrogen), 0.025% ascorbic acid (Sigma-Aldrich), and 10% FBS (Invitrogen), with or without BMS493 ($10^{-6}$ M) or all-*trans* RA ($10^{-7}$ M; Sigma-Aldrich), as described previously (30, 32). Similarly, E11.5 mouse lungs were cultured for 24 to 48 hours in the same media as above, with or without BMS493. Specimens were processed for qPCR, Western blotting, ISH, IHC, or X-gal staining, as reported previously (36, 65).

*Microarray analysis*. E8.5 WT (control and BMS493-treated) and *Aldh1a2*-null (control and RA-treated) foreguts were cultured for 24 hours. RNA was isolated (RNeasy; QIAGEN) and processed for microarray analysis (Affymetrix Mouse Genome 430 2.0 array chip). Gene expression profiles were compared, and the difference was considered significant if the *P* value was less than 0.05 (Cyber-T software) (32).

*Dietary manipulation of vitamin A*. Nonpregnant mice were maintained on a standard nutritionally complete VAS chow diet (15 IU of vitamin A/g of diet; irradiated Teklad Global 18% Protein Rodent Diet 2018). All pregnant females were given a VAS diet initially until 9.5 dpc, then randomized to (a) the VAS diet, or (b) the VAD diet (<0.2 IU of vitamin A/g of diet; irradiated Mod TestDiet AIN-93M/no vitamin A). 14.5 dpc, females were either sacrificed for embryonic lung analyses or allowed to continue on a VAS diet.

*HPLC analysis of retinoids*. Reverse-phase HPLC analysis of ROH and RE was performed as described (66). Mouse lungs were frozen on dry ice, shielded from light, and processed. ROH and RE were separated and identified by comparing retention times and spectral data of experimental compounds with those of authentic standards. ROH and RE concentrations were quantified by comparing peak integrated areas of unknowns against those of purified standards.

*Whole-mount detection of β-gal activity (X-gal staining)*. Lungs and lung explants were fixed for 5 minutes in 0.25% glutaraldehyde containing 2 mM $MgCl_2$ and placed in the X-gal solution overnight at room temperature, as reported previously (36).

*qPCR and Western blot analysis*. For qPCR, total RNA was reverse transcribed with SuperScript III (QIAGEN) and amplified using TaqMan (Applied Biosystems); β-actin (*Actb*) mRNA was used as an internal control. For Western blotting, protein extracts were subjected to SDS-PAGE, blotted onto nitrocellulose, incubated overnight with primary antibodies in Tris-buffered saline with 0.1% Tween-20 and 5% milk (Ki67, 1:500, Abcam; SM22α and SMMHC2, 1:1,000, Abcam; pMYL2 and tMYL2, 1:1,000, Cell Signaling Technology), and developed (SuperSignal West Pico; Thermo Scientific). Results were normalized to GAPDH (1:5,000; R&D Systems) and quantified using ImageJ software (NIH).

*Histology, IHC, and ISH*. Tissue sections were stained with H&E or Masson's trichrome (Sigma-Aldrich) using protocols provided by the manufac-

turers. For IHC, sections were incubated with HRP- or AP-conjugated antibodies (α-SMA, 1:1,000, Santa Cruz Biotechnology Inc.; SM22α, 1:1,000, Abcam; SMMHC2, 1:1,000, Abcam; and Ki67, 1:200, Cell Signaling Technology) and developed using kits and protocols provided by Vector Laboratories. ISH was performed in 96-well plates (whole-mount specimens) or in 5-μm paraffin sections, as reported previously (32).

*Isolation and sorting of Acta2-GFP–positive cells*. Cell suspensions were obtained by digesting lungs and lung explants with 0.1% collagenase A (Roche Diagnostics), 2.4 units/ml dispase (Roche Diagnostics), and 6 units/ml DNase I (QIAGEN) at 37°C for 1 hour. GFP-positive cells were collected using a MoFlo cell sorter (Beckman Coulter). The GFP-positive cells were then processed for qPCR and Western blotting.

*Morphometry*. α-SMA IHC images of lungs from WT and DKO mice (×20 and ×40 magnification) were analyzed with ImageJ software following established protocols (67). α-SMA–labeled airway SM cells were counted in 15 large- and 15 medium-sized airways and normalized to the surface of their basement membranes. The intensity of the α-SMA signals was estimated by changing images to 8-bit grayscale and determining the mean gray value of the IHC signal in 15 random regions around the airways sampled by the ImageJ oval tool, excluding the vasculature. Background subtraction was done by sampling 15 random, α-SMA–negative regions from the same lung. The volume occupied by the αSMA–positive cells in the airways was outlined (freehand tool), and the value was expressed per SA of the associated basement membrane.

*Methacholine challenge and airway resistance measurements*. Adult mice were anesthetized and paralyzed (i.p. pentobarbital, 100 μg/g BW; pancuronium, 0.5 μg/g BW), intubated (tracheostomy), placed on a mechanical ventilator (flexiVent; SCIREQ), and ventilated at 300 breaths/minute (tidal volume: 6–7 ml/kg; 3 cm $H_2O$ positive end expiratory pressure [PEEP]). Baseline airway resistance and elastance were measured after airway delivery of nebulized vehicle (0 mg/ml of methacholine) and, thereafter, with delivery of increasing concentrations of nebulized methacholine (5 and 10 mg/ml) (53). Lungs were then harvested and processed for various analyses. flexiVent data were presented as absolute airway resistance (Rn) and relative resistance from baseline.

*Statistics*. Statistical analyses were performed using 2-tailed Student's *t* tests (minimum of three samples per condition). Differences were considered significant if the *P* value was less than 0.05.

*Study approval*. All experiments involving animals were performed according to protocols approved by the IACUC of Boston University.

## Acknowledgments

We are indebted to Pascal Dollé, Karen Niederreither, and Janet Rossant for providing the *Aldh1a2*-null and *RARElacZ* reporter mouse lines; Anne Hinds for her help with histology; Kavon Kaboli for her assistance with flexiVent analysis; and Jining Lü, Xingbin Ai, Matt Layne, and Yuxia Cao for their thoughtful discussions. This work was supported by grants from the NIH (R01 HL067129-09 and R01 HD057493).

Received for publication April 3, 2013, and accepted in revised form October 30, 2013.

Address correspondence to: Wellington V. Cardoso, Columbia Center for Human Development, Department of Medicine, Columbia University Medical Center, 650 West 168th Street, Room BB 8-812, New York, New York 10032, USA. Phone: 212.305.7310; Fax: 671.536.8093; E-mail: wvc2104@columbia.edu.

1. West KP, Howard GR, Sommer A. Vitamin A and infection: public health implications. *Annu Rev Nutr*. 1989;9:63–86.
2. West KP Jr. Extent of vitamin A deficiency among preschool children and women of reproductive age. *J Nutr*. 2002;132(9 Suppl):2857S–2866S.
3. Williams SR. *Nutrition and Diet Therapy: Instructor's Manual and Text Book*. Maryland Heights, Missouri, USA: Mosby; 1997.
4. Chambon P. The retinoid signaling pathway: molecular and genetic analyses. *Semin Cell Biol*. 1994;5(2):115–125.
5. Clagett-Dame M, DeLuca HF. The role of vitamin a in mammalian reproduction and embryonic development. *Annu Rev Nutr*. 2002;22:347–381.
6. Wilson JG, Roth CB, Warkany J. An analysis of the syndrome of malformations induced by maternal vitamin A deficiency. Effects of restoration of vitamin A at various times during gestation. *Am J Anat*. 1953;92(2):189–217.
7. Spears K, Cheney C, Zerzan J. Low plasma retinol concentrations increase the risk of developing bronchopulmonary dysplasia and long-term respiratory disability in very-low-birth-weight infants. *Am J Clin Nutr*. 2004;80(6):1589–1594.
8. Babu TA, Sharmila V. Vitamin A supplementation in late pregnancy can decrease the incidence of bronchopulmonary dysplasia in newborns. *J Matern Fetal Neonatal Med*. 2010;23(12):1468–1469.
9. Kling DE, Schnitzer JJ. Vitamin A deficiency (VAD), teratogenic, and surgical models of congenital diaphragmatic hernia (CDH). *Am J Med Genet C Semin Med Genet*. 2007;145C(2):139–157.
10. Golzio C, et al. Matthew-Wood syndrome is caused by truncating mutations in the retinol-binding protein receptor gene STRA6. *Am J Hum Genet*. 2007; 80(6):1179–1187.
11. Arora P, Kumar V, Batra S. Vitamin A status in children with asthma. *Pediatr Allergy Immunol*. 2002;13(3):223–226.
12. Luo Z-X, et al. Vitamin A deficiency and wheezing. *World J Pediatr*. 2010;6(1):81–84.
13. Allen S, Britton JR, Leonardi-Bee JA. Association between antioxidant vitamins and asthma outcome measures: systematic review and meta-analysis. *Thorax*. 2009;64(7):610–619.
14. Al Senaidy AM. Serum vitamin A and beta-carotene levels in children with asthma. *J Asthma*. 2009; 46(7):699–702.
15. Checkley W, et al. Maternal vitamin A supplementation and lung function in offspring. *N Engl J Med*. 2010;362(19):1784–1794.
16. Patelarou E, et al. Association between biomarker-quantified antioxidant status during pregnancy and infancy and allergic disease during early childhood: a systematic review. *Nutr Rev*. 2011; 69(11):627–641.
17. Badri KR, Zhou Y, Schuger L. Embryological origin of airway smooth muscle. *Proc Am Thorac Soc*. 2008;5(1):4–10.
18. Tollet J, Everett AW, Sparrow MP. Spatial and temporal distribution of nerves, ganglia, and smooth muscle during the early pseudoglandular stage of fetal mouse lung development. *Dev Dyn*. 2001;221(1):48–60.
19. Sparrow MP, Lamb JP. Ontogeny of airway smooth muscle: structure, innervation, myogenesis and function in the fetal lung. *Respir Physiol Neurobiol*. 2003;137(2–3):361–372.
20. Peng T, et al. Coordination of heart lung co-development by a multipotent cardiopulmonary progenitor. *Nature*. 2013;500(7464):589–592.
21. Schittny JC, Miserocchi G, Sparrow MP. Spontaneous peristaltic airway contractions propel lung liquid through the bronchial tree of intact and fetal lung explants. *Am J Respir Cell Mol Biol*. 2000; 23(1):11–18.
22. Jesudason EC, et al. Developing rat lung has a sided pacemaker region for morphogenesis-related airway peristalsis. *Am J Respir Cell Mol Biol*. 2005; 32(2):118–127.
23. Hirota JA, Nguyen TT, Schaafsma D, Sharma P, Tran T. Airway smooth muscle in asthma: phenotype plasticity and function. *Pulm Pharmacol Ther*. 2009;22(5):370–378.
24. Zuyderduyn S, Sukkar MB, Fust A, Dhaliwal S, Burgess JK. Treating asthma means treating airway smooth muscle cells. *Eur Respir J*. 2008;32(2):265–274.
25. Mizuno Y, Furusho T, Yoshida A, Nakamura H, Matsuura T, Eto Y. Serum vitamin A concentrations in asthmatic children in Japan. *Pediatr Int*. 2006;48(3):261–264.
26. DiCosmo BF, et al. Airway epithelial cell expression of interleukin-6 in transgenic mice. Uncoupling of airway inflammation and bronchial hyperreactivity. *J Clin Invest*. 1994;94(5):2028–2035.
27. Plant PJ, et al. Hypertrophic airway smooth muscle mass correlates with increased airway responsiveness in a murine model of asthma. *Am J Respir Cell Mol Biol*. 2012;46(4):532–540.
28. Niederreither K, Subbarayan V, Dollé P, Chambon P. Embryonic retinoic acid synthesis is essential for early mouse post-implantation development. *Nat Genet*. 1999;21(4):444–448.
29. Dickman ED, Thaller C, Smith SM. Temporally-regulated retinoic acid depletion produces specific neural crest, ocular and nervous system defects. *Dev Camb Engl*. 1997;124(16):3111–3121.
30. Desai TJ, Malpel S, Flentke GR, Smith SM, Cardoso WV. Retinoic acid selectively regulates Fgf10 expression and maintains cell identity in the prospective lung field of the developing foregut. *Dev Biol*. 2004;273(2):402–415.
31. Desai TJ, et al. Distinct roles for retinoic acid receptors alpha and beta in early lung morphogenesis. *Dev Biol*. 2006;291(1):12–24.
32. Chen F, Desai TJ, Qian J, Niederreither K, Lü J, Cardoso WV. Inhibition of Tgfβ signaling by endoge-

nous retinoic acid is essential for primary lung bud induction. *Development*. 2007;134(16):2969–2979.
33. Chen F, Cao Y, Qian J, Shao F, Niederreither K, Cardoso WV. A retinoic acid-dependent network in the foregut controls formation of the mouse lung primordium. *J Clin Invest*. 2010;120(6):2040–2048.
34. Manabe I, Nagai R. Regulation of smooth muscle phenotype. *Curr Atheroscler Rep*. 2003;5(3):214–222.
35. Rossant J, Zirngibl R, Cado D, Shago M, Giguère V. Expression of a retinoic acid response element-hsplacZ transgene defines specific domains of transcriptional activity during mouse embryogenesis. *Genes Dev*. 1991;5(8):1333–1344.
36. Malpel S, Mendelsohn C, Cardoso WV. Regulation of retinoic acid signaling during lung morphogenesis. *Development*. 2000;127(14):3057–3067.
37. Kong SK, Halayko AJ, Stephens NL. Increased myosin phosphorylation in sensitized canine tracheal smooth muscle. *Am J Physiol - Lung Cell Mol Physiol*. 1990;259(2):L53–L56.
38. Jean J-C, Lü J, Joyce-Brady M, Cardoso WV. Regulation of Fgf10 gene expression in murine mesenchymal cells. *J Cell Biochem*. 2008;103(6):1886–1894.
39. Chazaud C, Dollé P, Rossant J, Mollard R. Retinoic acid signaling regulates murine bronchial tubule formation. *Mech Dev*. 2003;120(6):691–700.
40. Mailleux AA, et al. Fgf10 expression identifies parabronchial smooth muscle cell progenitors and is required for their entry into the smooth muscle cell lineage. *Development*. 2005;132(9):2157–2166.
41. Cardoso WV, Lü J. Regulation of early lung morphogenesis: questions, facts and controversies. *Development*. 2006;133(9):1611–1624.
42. Warburton D, et al. Lung organogenesis. *Curr Top Dev Biol*. 2010;90:73–158.
43. Wang D, et al. Activation of cardiac gene expression by myocardin, a transcriptional cofactor for serum response factor. *Cell*. 2001;105(7):851–862.
44. Goss AM, et al. Wnt2 signaling is necessary and sufficient to activate the airway smooth muscle program in the lung by regulating myocardin/Mrtf-B and Fgf10 expression. *Dev Biol*. 2011;356(2):541–552.
45. Wang D-Z, et al. Potentiation of serum response factor activity by a family of myocardin-related transcription factors. *Proc Natl Acad Sci U S A*. 2002; 99(23):14855–14860.
46. Ghosh S, et al. Activation dynamics and signaling properties of Notch3 receptor in the developing pulmonary artery. *J Biol Chem*. 2011; 286(25):22678–22687.
47. Kim Y-K, et al. Retinyl ester formation by lecithin: retinol acyltransferase is a key regulator of retinoid homeostasis in mouse embryogenesis. *J Biol Chem*. 2008;283(9):5611–5621.
48. Morrisey EE, Hogan BLM. Preparing for the first breath: genetic and cellular mechanisms in lung development. *Dev Cell*. 2010;18(1):8–23.
49. Kim Y-K, Quadro L. Reverse-phase high-performance liquid chromatography (HPLC) analysis of retinol and retinyl esters in mouse serum and tissues. *Methods Mol Biol*. 2010;652:263–275.
50. Tompkins DH, et al. Sox2 is required for maintenance and differentiation of bronchiolar Clara, ciliated, and goblet cells. *PLoS One*. 2009;4(12):e8248.
51. Que J, Luo X, Schwartz RJ, Hogan BLM. Multiple roles for Sox2 in the developing and adult mouse trachea. *Dev Camb Engl*. 2009;136(11):1899–1907.
52. Lu Y, Okubo T, Rawlins E, Hogan BLM. Epithelial progenitor cells of the embryonic lung and the role of microRNAs in their proliferation. *Proc Am Thorac Soc*. 2008;5(3):300–304.
53. Little FF, de Bie J, van Oosterhout A, Kornfeld H, Center DM, Cruikshank WW. Immunomodulatory effect of interleukin-16 on allergic airway inflammation. *Chest*. 2003;123(3 Suppl):431S–432S.
54. Rensen SS, Doevendans PA, van Eys GJ. Regulation and characteristics of vascular smooth muscle cell phenotypic diversity. *Neth Heart J*. 2007; 15(3):100–108.
55. Azambuja AP, et al. Retinoic acid and VEGF delay smooth muscle relative to endothelial differentiation to coordinate inner and outer coronary vessel wall morphogenesis. *Circ Res*. 2010;107(2):204–216.
56. Weaver M, Batts L, Hogan BL. Tissue interactions pattern the mesenchyme of the embryonic mouse lung. *Dev Biol*. 2003;258(1):169–184.
57. Litingtung Y, Lei L, Westphal H, Chiang C. Sonic hedgehog is essential to foregut development. *Nat Genet*. 1998;20(1):58–61.
58. Pepicelli CV, Lewis PM, McMahon AP. Sonic hedgehog regulates branching morphogenesis in the mammalian lung. *Curr Biol*. 1998;8(19):1083–1086.
59. Cohen ED, Ihida-Stansbury K, Lu MM, Panettieri RA, Jones PL, Morrisey EE. Wnt signaling regulates smooth muscle precursor development in the mouse lung via a tenascin C/PDGFR pathway. *J Clin Invest*. 2009;119(9):2538–2549.
60. Yi L, Domyan ET, Lewandoski M, Sun X. Fibroblast growth factor 9 signaling inhibits airway smooth muscle differentiation in mouse lung. *Dev Dyn*. 2009;238(1):123–137.
61. McGowan SE, et al. Vitamin A deficiency promotes bronchial hyperreactivity in rats by altering muscarinic M(2) receptor function. *Am J Physiol Lung Cell Mol Physiol*. 2002;282(5):L1031–L1039.
62. Barker DJ. In utero programming of chronic disease. *Clin Sci (Lond)*. 1998;95(2):115–128.
63. Håland G, et al. Reduced lung function at birth and the risk of asthma at 10 years of age. *N Engl J Med*. 2006;355(16):1682–1689.
64. Demarini DM, Preston RJ. Smoking while pregnant: Transplacental mutagenesis of the fetus by tobacco smoke. *JAMA*. 2005;293(10):1264–1265.
65. Lü J, Qian J, Izvolsky KI, Cardoso WV. Global analysis of genes differentially expressed in branching and non-branching regions of the mouse embryonic lung. *Dev Biol*. 2004;273(2):418–435.
66. Quadro L, et al. Impaired retinal function and vitamin A availability in mice lacking retinol-binding protein. *EMBO J*. 1999;18(17):4633–4644.
67. Kotlikoff MI, et al. Methodologic advancements in the study of airway smooth muscle. *J Allergy Clin Immunol*. 2004;114(2 suppl):S18–S31.